Send Orders for Reprints to reprints@benthamscience.net

Current Alzheimer Research, **2014**, *11*, **389-398**

Altered Amplitude of Low-frequency Fluctuations in Early and Late Mild Cognitive Impairment and Alzheimer's Disease

Peipeng Liang[1,2,3,#], Jie Xiang[4,#], Hong Liang[4], Zhigang Qi[1,2,3], Kuncheng Li[1,2,3,*], Alzheimer's Disease NeuroImaging Initiative

[1]*Department of Radiology, Xuanwu Hospital, Capital Medical University, Beijing 100053, China;* [2]*Beijing Key Laboratory of Magnetic Resonance Imaging and Brain Informatics, Beijing 100053, China;* [3]*Key Laboratory for Neurodegenerative Diseases, Ministry of Education, PR China;* [4]*Department of Computer Science and Technology, Taiyuan University of Technology, Taiyuan 030024,China*

Abstract: *Purpose*: Previous studies have shown that the strength of the low frequency fluctuation in the medial-line brain areas are abnormally reduced in mild cognitive impairment (MCI) and Alzheimer's disease (AD) patients. The purpose of this study was to explore the functional brain changes in early MCI (EMCI) and late MCI (LMCI) patients by measuring the amplitude of the blood oxygenation level dependent (BOLD) functional MRI (fMRI) signals at rest. *Materials and methods*: 35 elderly normal controls (NC), 24 EMCI, 29 LMCI, and 14 AD patients from the Alzheimer's Disease Neuroimaging Initiative (ADNI2) were included in this study. Resting state fMRI and 3D structural MRI data were acquired. The spatial patterns of spontaneous brain activity were measured by examining the amplitude of low-frequency fluctuations (ALFF) of BOLD signal during rest. A one-way analysis of variance (ANOVA) was then performed on ALFF maps, with age, sex and regional atrophy as covariates. *Results*: There were widespread ALFF differences among the four groups. As compared with controls, AD, LMCI and EMCI patients showed decreased ALFF mainly in the posterior cingulate cortex, precuneus, right lingual gyrus and thalamus (with a linear trend: NC>EMCI>LMCI>AD), while there was increased activity in the right parahippocampal gyrus (with a linear trend: NC<EMCI<LMCI<AD). Additionally, we also showed that many regions with ALFF changes had significant correlations with the cognitive performance as measured by mini-mental state examination scores (MMSE) and the emotion states as measured by Geriatric Depression Scale (GD scale) for EMCI, LMCI and AD patients, but not for controls. *Conclusion*: Our results indicated that the significantly altered ALFF activities can be detected at EMCI stage, independent of age, sex and regional atrophy. The present study thus suggests ALFF abnormalities as a potential biomarker for the early diagnosis of AD and further provides insights into biological mechanisms of the diseases.

Keywords: Alzheimer's disease (AD), early mild cognitive impairment (EMCI), functional MRI, late MCI, resting state.

INTRODUCTION

Alzheimer's disease (AD) is the most prevalent form of dementia worldwide with symptoms of global cognitive decline, including progressive loss of memory, reasoning and language [1]. Early diagnosis and early intervention of AD may be necessary and helpful, not only because the patient's level of function will be preserved for a longer period, but also because community-dwelling patients with AD incur less societal cost than those who require long-term institutional placement [2]. Mild cognitive impairment (MCI) is an intermediate state between healthy aging and AD, with a higher risk of developing dementia [3]. In the attempt to define an even earlier point in time for disease detection, the recent extensions of the Alzheimer's disease neuroimaging initiative (ADNI), i.e., ADNI Go study and ADNI 2, have introduced the distinction of MCI into early and late MCI. Late MCI (LMCI) refers to the original definition (performance of 1.5 standard derivations (SD) below the normative mean), whereas in early MCI (EMCI), impairment is defined as performance between 1.0 SD and 1.5 SD below the normative mean on a standard test [4, 5]. There have been many anatomical and functional neuroimaging studies of MCI and AD in order to search for biomarkers of early diagnosis (see reviewers in [6, 7]). However, neuroimaging studies of EMCI and LMCI patients are still less.

Resting state functional magnetic resonance imaging (rs-fMRI) has been widely used in the early diagnosis of MCI and AD (see a review: [8]), and has been demonstrated to be more effective at identifying functional pathology as compared to task-fMRI techniques [9]. Several rs-fMRI studies using amplitude of low frequency fluctuation (ALFF) [10, 11] measures have identified abnormalities of low frequency oscillations (LFO, 0.01-0.08 Hz) in many brain regions, and suggested using ALFF as a potentially useful tool for understanding the pathophysiology of amnesic MCI (aMCI) and AD. For example, Han *et al.* [12] compared healthy elder with aMCI patients and reported that aMCI had decreased ALFF values in the posterior cingulate cortex/precuneus

*Address correspondence to this author at the Xuanwu Hospital, Capital Medical University, 45 Chang Chun Street, Xi Cheng District, Beijing 100053, China; Tel: 86-10-83198376; Fax: 86-10-83198376;
E-mail: cjr.likuncheng@vip.163.com

1875-5828/14 $58.00+.00

(PCC/PCu), medial prefrontal cortex (MPFC), hippocampus/parahippocampal gyrus (PHG), basal ganglia, and prefrontal regions, and increased ALFF values mainly in several occipital and temporal regions. Xi *et al.* [13] compared healthy elder with mild AD patients and found that the mild AD showed decreased ALFF in the right PCC, ventral medial prefrontal cortex (VMPFC) and the bilateral dorsal medial prefrontal cortex (DMPFC), as well as increased ALFF in some regions. In an additional study, three groups of participants were compared, i.e., healthy elderly, MCI and AD [14]. They found that AD and MCI patients showed abnormal ALFF in various brain regions of the frontal, temporal, and parietal lobes, among which PCC showed the most significant group differences with a trend of AD < MCI < healthy elderly.

The purpose of the present study was to repeat the above studies on ALFF alterations in MCI and AD. More importantly, it aimed to assess ALFF difference between EMCI and LMCI, which has not been characterized before. Given that many previous studies have commonly demonstrated decreased spontaneous PCC activity [15-20], specifically, reduced ALFF [12-14], in both AD and MCI/aMCI, we hypothesized that the patients with EMCI, LMCI and AD would show abnormal LFO amplitudes in this region and may follow a linear trend of AD<LMCI<EMCI<controls. In addition, we also expected to find EMCI, LMCI, and AD-related ALFF changes in other brain regions.

MATERIALS AND METHODS

Participants

The 102 participants in this study were recruited between 2011 and 2013 through ADNI-2 from 56 centers in the USA and Canada (Table **1**). Written consent was obtained from all subjects participating in the study, and the study was approved by the institutional review board at each participating site. Inclusion/exclusion criteria for ADNI studies are described elsewhere (https://ida.loni.ucla.edu/login.jsp?project=ADNI).

From the ADNI-2 dataset, we selected all participants between 55-90 (inclusive) years of age who had completed, in the same visit, the following imaging assessments: MRI (3D MPRAGE) and resting state fMRI. Although neuropsychological assessments were not used as the requisites for search, most of participants were tested with Mini-mental State Examination (MMSE), Global Clinical Dementia Rating (Global CDR), Neuropsychiatric Inventory Questionnaire (NPI-Q), Geriatric Depression Scale (GD Scale), as well as Functional Assessment Questionnaire (FAQ). Selected individuals were classified as normal controls (NC), EMCI, LMCI and AD according to clinical and behavioral measures provided by ADNI2 at the time of the imaging study. Individuals with modified Hachinski Ischemia score higher than four points were excluded during the screening phase. Furthermore, subjects with imaging evidence of clinically significant vascular changes were excluded from this analysis.

MRI Data Acquisition

Scans were acquired on 3.0T Philips MR scanners. The subjects were instructed to hold still, keep their eyes open during the entire scan and focus on a point on the mirror or scanner. Functional images were collected axially by using an echo-planar imaging (EPI) sequence [repetition time (TR)/echo time (TE)/flip angle (FA) = 3000 ms/30 ms/80°, field of view (FOV): RL= 212 mm/AP = 198.75 mm/FH = 159 mm, voxel size: RL = 3.3125 mm/AP=3.3125 mm, slices = 48, thickness = 3.3125 mm, gap = 0 mm, bandwidth = 1886.2 Hz/pixel]. The scan lasted for 423 s and 140 scans were collected. 3D T1-weighted magnetization-prepared rapid gradient echo (MPRAGE) sagittal images were collected by using MPRAGE (sequence name) with the following parameters: TR = 6.8 ms, TE = 3.1 ms, minimum inversion time (TI) = 849.9592 ms, flip angle = 9°, field of view (FOV): RL= 204 mm/AP = 240 mm/FH = 256 mm, and slices = 170 yielding a voxel size of 1 × 1 × 1.2 mm^3 ,with the total scan duration of 546.7s or using 2-fold acceleration using the sensitivity-encoding (SENSE) parallel imaging with the following parameters: TR = 6.8 ms, TE = 3.1 ms, minimum inversion time (TI) = 827.6673 ms, flip angle = 9°, field of view (FOV): RL= 204 mm/AP = 253.125 mm/FH = 270 mm, and slices = 170 yielding a voxel size of 1.11 × 1.11 × 1.2 mm^3 ,with the total scan duration of 334.2s

FMRI Data Preprocessing

All analyses were conducted using Data Processing Assistant for Resting-State fMRI software (DPARSF) [21] and

Table 1. Demographics and clinical findings.

	AD	LMCI	EMCI	Controls	P value
Sex, female/male	8/6	11/18	11/13	17/18	0.67[a]
Age, year	76.5±7.3	73.2±7.3	72.8±6.6	74.3±5.9	0.36[b]
MMSE	20.9±3.90	27.1±2.3	28.1±1.5	28.9±1.6	<0.01[b]
Global CDR	0.8±0.3	0.5±0.1	0.5±0.1	0±0	<0.01[b]
NPI-Q	3.0±2.4	2.8±2.6	2.2±3.1	0.6±1.3	<0.01[b]
GD scale	1.0±0.9	1.8±2.4	2.8±3.1	0.7±1.0	<0.01[b]
FAQ	16.3±7.6	5.4±6.2	3.2±4.0	0.2±0.7	<0.01[b]

MMSE = Mini-mental State Examination; Global CDR = Global Clinical Dementia Rating; NPI-Q = Neuropsychiatric Inventory Questionnaire; GD Scale = Geriatric Depression Scale;, FAQ = Functional Assessment Questionnaire; values are means ± SD.

[a]The P value for gender distribution in the four groups was obtained by chi-square test.

[b]The P value were obtained by one-way analysis of variance tests.

statistical parametric mapping software package (SPM5, http://www.fil.ion.ucl.ac.uk/spm). The first 10 volumes of the functional images were discarded to allow the signal to reach equilibrium and participants' adaptation to the scanning noise. The remaining 130 fMRI images were first corrected for within-scan acquisition time differences between slices and then realigned to the first volume to correct for inter-scan head motion. One AD patient, one EMCI patient and four normal controls were excluded according to the criteria that head motion was restricted to less than 2 mm of displacement or 2 degrees of rotation in any direction. The individual structural image was co-registered to the mean functional image after motion correction using a linear transformation. The transformed structural images were then segmented into gray matter (GM), white matter (WM) and cerebrospinal fluid (CSF) by using a unified segmentation algorithm [22]. The motion corrected functional volumes were spatially normalized to the Montreal Neurological Institute (MNI) space and re-sampled to 3 mm isotropic voxels using the normalization parameters estimated during unified segmentation. Subsequently, the functional images were spatially smoothed with a Gaussian kernel of $4 \times 4 \times 4$ mm^3 full width at half maximum (FWHM) to decrease spatial noise. Following this, temporal filtering ($0.01 \text{ Hz} < f < 0.08 \text{ Hz}$) was applied to the time series of each voxel to reduce the effect of low-frequency drifts and high-frequency noise [23].

ALFF Analysis

ALFF was calculated using Resting-State fMRI Data Analysis Toolkit (http://resting-fmri.sourceforge.net) [24], and the calculation procedure was the same as that reported in previous studies [12, 14, 25]. For a given voxel, the filtered time series was first converted to the frequency domain using a Fast Fourier Transform. The square root of the power spectrum was computed and then averaged across 0.01-0.08 Hz. This averaged square root was termed ALFF at the given voxel [10]. To reduce the global effects of variability across participants, the ALFF of each voxel was divided by the global mean ALFF value for each subject, which reflects, in a given voxel, the degree of its raw ALFF value relative to the average ALFF value of the whole brain. All the ALFF computations were restricted in the mask where the mean GM intensity across all subjects were larger than 0.15 (for details, see the following "structural image analysis" section).

Structural Image Analysis

Brain atrophy may cause a partial volume effect in functional imaging techniques [26]. To control for the potential impact of atrophy on the functional results, a voxel-based morphometry (VBM) analysis of structural images was firstly performed. Individual structural images were co-registered to the mean functional images after motion correction using a linear transformation [27]. GM intensity maps were obtained by the unified segmentation algorithm [22] as described in "FMRI Data Preprocessing" section. Individual GM maps were further modulated to compensate for the effect of spatial normalization using a linear and nonlinear method. After spatially smoothing with a Gaussian kernel of 10 mm FWHM, a one-way analysis of covariance (ANCOVA) test was performed on the smoothed GM intensity maps, with age and sex as covariates. The resultant images were used to identify the brain regions with GM loss. The statistical threshold was set at $p < 0.001$ and cluster size > 540 mm^3, which corresponded to a corrected $p < 0.05$ (using the AlphaSim program with parameters: FWHM= 10 mm, within the GM mask).

Statistics

Distributions of age, MMSE, Global CDR, NPI-Q, GD scale and FAQ scores among the four groups were compared by using one-way analysis of variance (ANOVA), and chi-square test was applied to compare gender distributions.

Unless otherwise stated, all imaging statistical analyses were conducted by using software REST. To determine the effects of group, we performed a one-way ANCOVA on a voxel-by-voxel basis of ALFF maps, with age, sex and GM volume as covariates. Then, post hoc two-sample t-tests were performed to identify difference between each pair of groups by using the above-mentioned covariates (corrected $P<0.05$ based on AlphaSim. Brain regions showing significant group differences were identified as masks). For those clusters showing significant main effects between groups, region of interest (ROI) analysis were further performed on ALFF values of each cluster to shown the relative patterns.

Imaging-behavior Correlation

In order to determine whether the ALFF index varied with disease progression in EMCI, LMCI and AD patients, correlation analyses between the fitted ALFF index and each of the clinical variables (scores of MMSE, NPI-Q, GD Scale, and FAQ) were performed after regressing out age and gender effects.

RESULTS

There were no significant differences between NC, EMCI, LMCI and AD patients in gender and age, but the MMSE, Global CDR, NPI-Q, GD scale and FAQ scores were significantly different ($P < 0.01$) between the four groups, with a linear trend of AD<LMCI<EMCI<NC for MMSE and GD scale, and a reverse linear trend of AD>LMCI>EMCI>NC for Global CDR, NPI-Q and FAQ.

VBM Analysis

It was found that the four groups of participants had significant GM differences in bilateral hippocampus (BA 28/34), bilateral middle/inferior temporal gyrus (MTG/ITG, BA 20/21), bilateral insula (BA 13), bilateral inferior parietal lobule (IPL, BA 7/40), bilateral postcentral gyrus (PosCG, BA 1/2), right superior frontal gyrus (SFG, BA 9), right superior frontal medial cortex (SFMC, BA 9), right angular gyrus (AG, BA 7) and right precentral gyrus (PreCG, BA 6) (Table **2** and Fig. **1**). The global maximum was located in the right hippcampus.

ALFF Analysis

The ANOCVA analysis showed that the four groups had significant ALFF differences in the bilateral posterior cingulate cortex extending into calcarine sulcus (PCC/CS, BA 23/30/31), left precuneus/paracentral lobule (PCu/PCL, BA 5),

Table 2. Group differences of gray matter density among four groups (NC, EMCI, LMCI and AD) using ANOCVA, with age and sex as covariates.

Regions	BA	Cluster Size	Coordinate			*T*
			x	y	z	
Left Hippocampus	34	706	-22	-12	-16	13.97
Left Inferior Temporal Gyrus	20	48	-64	-32	-20	10.39
Left Middle Temporal Gyrus	21	43	-64	-44	-10	9.57
Left Insula	13	33	-42	-14	6	8.80
Left Posterior Cingulate Cortex	31	27	-12	-42	18	9.99
Left Inferior Parietal Lobule	7	119	-34	-62	50	12.59
Left Inferior Parietal Lobule	40	37	-54	-42	50	10.50
Left Postcentral Gyrus	2	24	-40	-36	64	10.31
Left Cerebellum		20	-20	-48	-42	9.62
Right Superior Frontal Medial Cortex	9	44	10	54	46	10.34
Right Superior Frontal Gyrus	9	21	22	44	38	10.00
Right Hippocampus	28	1934	34	-22	-16	25.42
Right Inferior Temporal Gyrus	21	178	46	2	-42	14.83
Right Middle Temporal Gyrus	21	127	60	-8	-14	11.29
Right Middle Temporal Gyrus	21	530	66	-28	-16	13.59
Right Insula	13	32	40	14	2	9.92
Right Postcentral Gyrus	1	37	58	-18	48	9.47
Right Angular Gyrus	7	65	34	-70	50	9.98
Right Precentral Gyrus	6	42	54	-6	50	12.36
Right Inferior Parietal Lobule	40	94	52	-38	52	13.10

right cingulate gyrus (CG, BA 32), right PCu (BA 31), right lingual gyrus (LG, BA19), right parahippocampal gyrus (PHG, BA 36) and right thalamus (Table **3** and Fig. **2**). Table **S1** in the supplemental material showed the results of the post-hoc pair-wise comparisons.

We further defined the nine clusters identified in the previous ANOCVA analysis as ROIs (Table **3** and Fig. **2**). The fitted ALFF values of each ROI were shown in (Fig. **3**). For the right FG, there is a trend of AD>LMCI>EMCI>NC, while the trends are AD<LMCI<EMCI<NC for the other eight ROIs.

Correlations Between ALFF and Neuropsychological Measures

As shown in (Fig. **4**), GD scale was negatively correlated with ALFF in right thalamus (r=-0.535, p=0.002) and left PCu/PCL (r=-0.504, p=0.004) for LMCI, and near to be significantly correlated with ALFF in right thalamus (r=-0.536, p=0.006) for EMCI. As shown in (Fig. **5-7**), MMSE is significantly correlated with ALFF in many regions for patients but not for controls. (Fig. **5**) showed that MMSE was positively correlated with ALFF in right PCu (r=0.745, p=0.003) and PCC (r=0.714, p=0.005) for AD. (Fig. **6**) showed that MMSE was positively correlated ALFF in right LG (r=0.500, p=0.004), left PCC/CS (r=0.546, p=0.002), right PCC/CS (r=0.542, p=0.002), right thalamus (r=0.488, p=0.005), right PCu (r=0.557, p=0.001), right PCC (r=0.576, p=0.001) and right PCu/PCL (r=0.516, p=0.003) for LMCI. (Fig. **7**) showed that MMSE was negatively correlated with ALFF in right PHG (r=-0.590, p=0.003), and positively correlated with ALFF in right PCC/CS (r=0.613, p=0.002), right PCu (r=0.595, p=0.003) and right PCC (r=0.610, p=0.002) for EMCI. The P values were corrected for multiple comparison using Bonferroni test (P<0.05/9; as shown in Table **3**, 9 clusters were identified.). All the other correlations were not significant. Additionally, both in patients and controls, neither ROI was correlated with NPI-Q and FAQ.

DISCUSSION

The novelty of the present study lies in the fact that we investigate the intrinsic or spontaneous brain activity changes in EMCI, LMCI and AD by measuring the ALFF values of rs-fMRI signals. This may add to the efforts to the

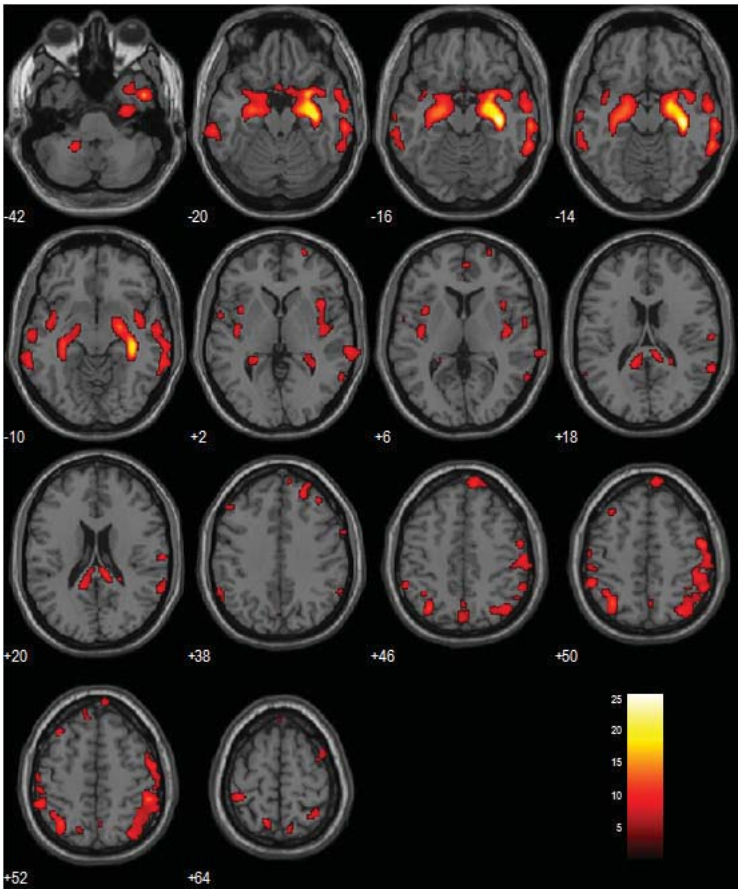

Fig. (1). Maps of GM volume differences among the EMCI, LMCI, AD, and healthy controls using a voxel-based-mophometry method. The statistical threshold was set at a corrected $p<0.05$ using the AlphaSim method.

Table 3. ALFF Group differences of four groups (NC, EMCI, LMCI and AD) using ANOCVA, with age, sex and structural atrophy as covariates.

Regions	BA	Cluster Size	Coordinate			*T*
			x	y	z	
Left Posterior Cingulate Cortex/Calcarine Sulcus	30	80	-12	-60	9	8.02
Left Precuneus/Paracentral Lobule	5	145	0	-42	54	8.77
Right Posterior Cingulate Cortex/Calcarine Sulcus	31	259	9	-72	21	9.77
Right Cingulate Gyrus	32	83	6	9	39	8.60
Right Precuneus	31	22	18	-54	24	7.97
Right Posterior cingulate Cortex	23	127	-3	-33	27	8.76
Right Thalamus		106	15	-9	12	7.00
Right Lingual Gyrus	19	37	15	-45	-6	7.11
Right Parahippocampal Gyrus	36	39	36	-36	-15	10.91

early diagnosis of AD. We found that there were significant differences in ALFF values among the EMCI, LMCI and AD patients, and healthy elderly in cingulate regions, thalamus, parahippocampal gyrus (PHG) and lingual gyrus (LG). Of these, increased ALFF values were observed in all three groups of patients in the right PHG regions. In contrast, decreased ALFF values were mainly observed in default mode network (DMN) regions (mainly including posterior cingulate cortex (PCC), precuneus (PCu)), right thalamus and right LG. Specifically, the most significant ALFF difference

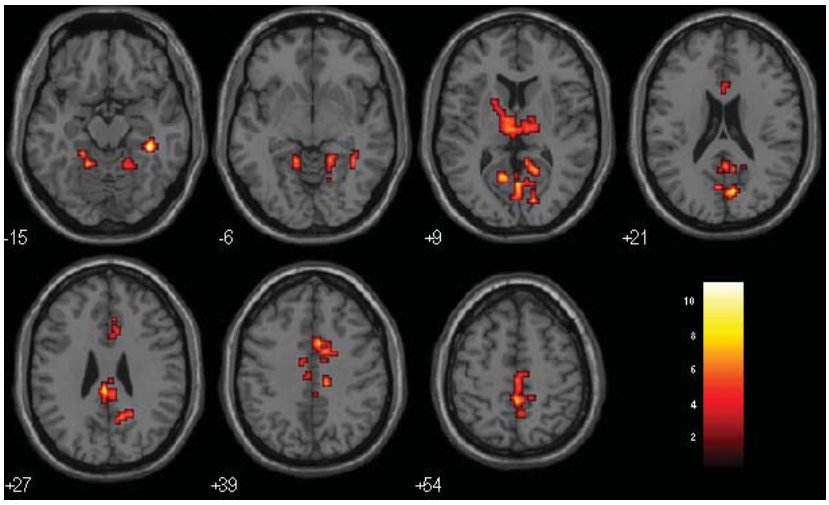

Fig. (2). ALFF statistical maps with group differences. These regions are identified by ANOVCA, with age, sex, and structural atrophy as covariates. The statistical threshold was set at a corrected p<0.05 using the AlphaSim method.

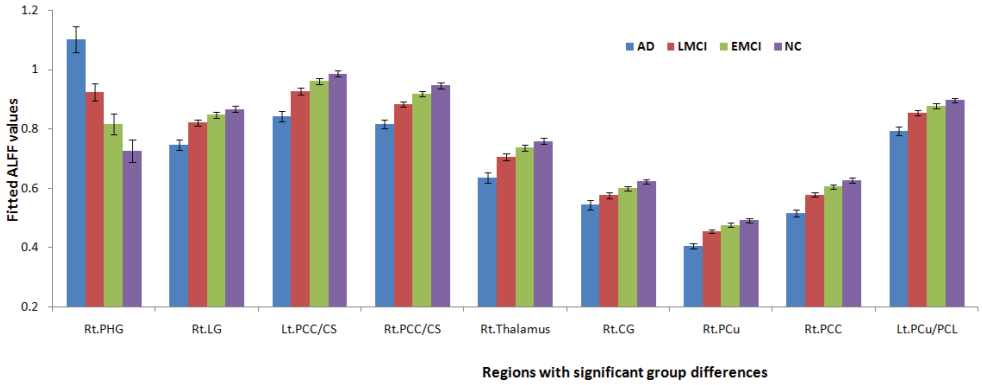

Fig. (3). Fitted ALFF values of nine regions with significant group differences among four groups (NC, EMCI, LMCI and AD). (See Table **S2**) in the supplemental material for statistical p values of pair-wise comparisons. These regions are identified by ANOVCA, with age, sex, and structural atrophy as covariates. Right Paraphippocampal Gyrus = Rt. PHG; Right Lingual Gyrus = Rt.LG; Left Posterior Cingulate Cortex/Calcarine Sulcus = Lt.PCC/CS; Right Posterior Cingulate Cortex/Calcarine Sulcus = Rt. PCC/CS; Right Cingulate Gyrus = Rt.CG; Right Precuneus = Rt.Pcu; Right Posterior Cingulate Cortex = Rt.PCC; Left Precuneus/Paracentral Lobule/ = Lt.PCu/PCL.

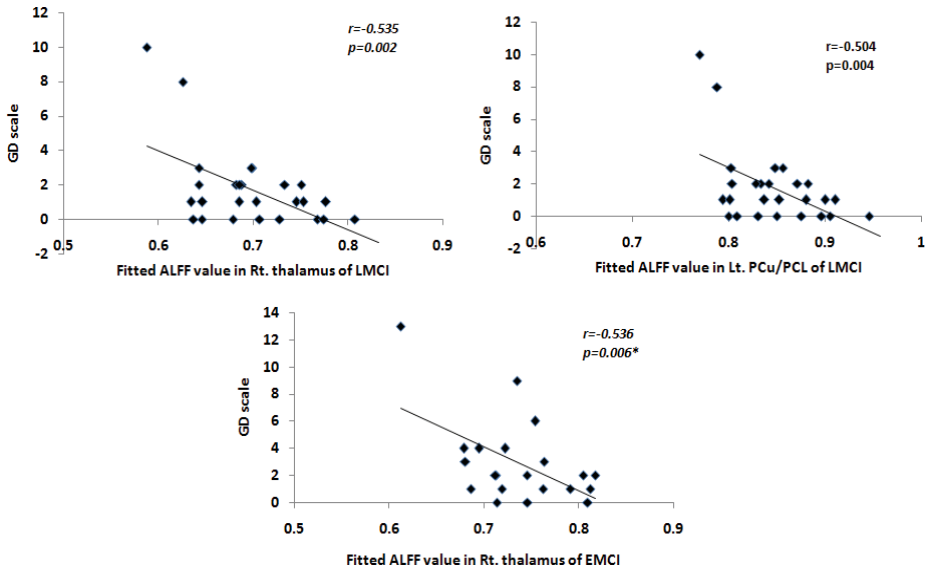

Fig. (4). GD scale score showed negative correlation with ALFF values in the right thalamus and PCu/PCL for LMCI patients, and in the right thalamus for EMCI patients.

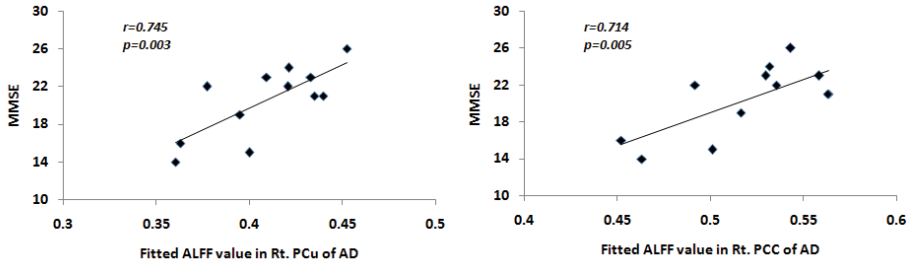

Fig. (5). ALFF in the right PCu and PCC showed significantly positive correlation with MMSE for AD patients.

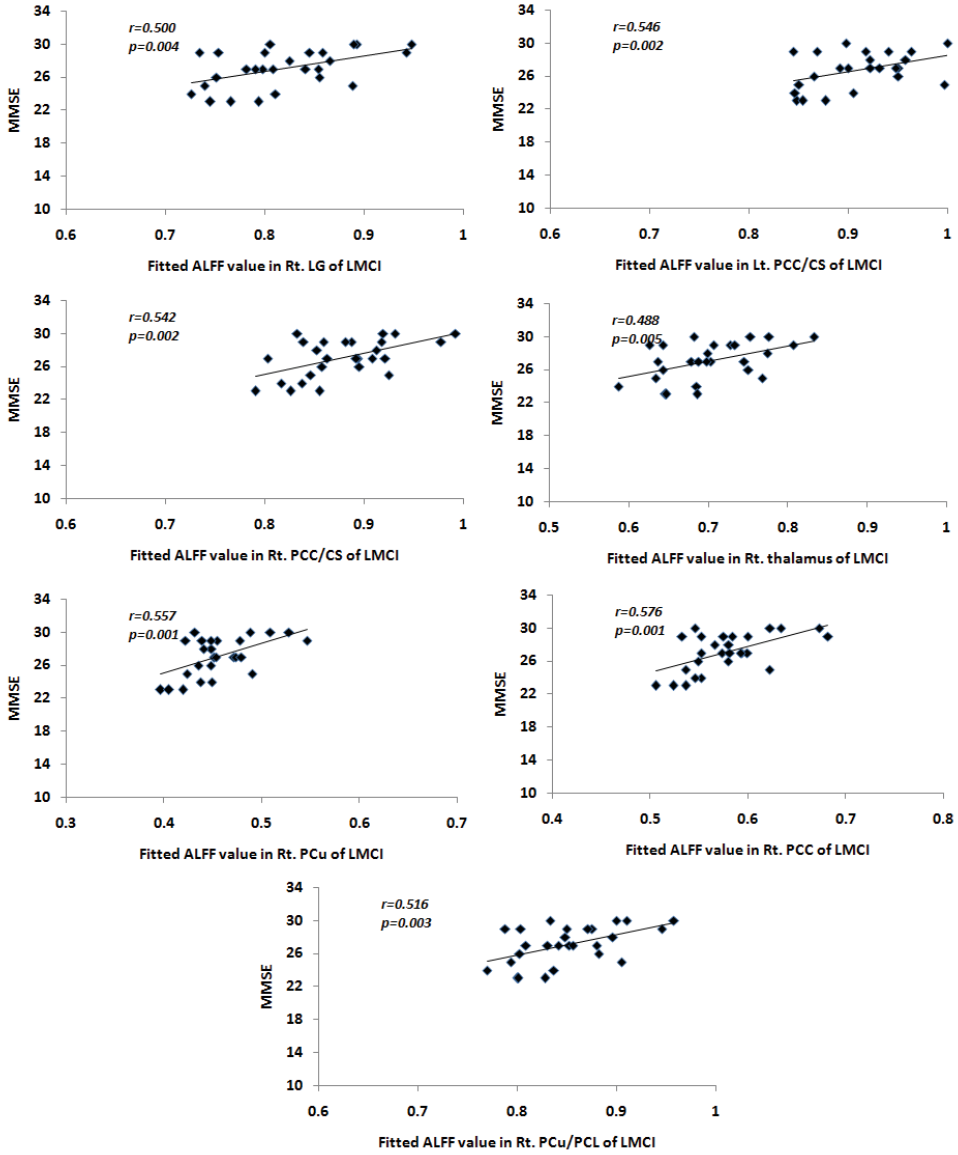

Fig. (6). ALFF in seven clusters located at the right LG, thalamus, PCu, PCC and bilateral PCC/CS showed significantly positive correlation with MMSE for LMCI patients.

among the four groups appeared in the right PCC extending into calcarine sulcus (CS), and both the increased and the decreased ALFF in the previous brain regions followed a general linear pattern of AD < LMCI < EMCI < NC or AD > LMCI > EMCI > NC. We also found that many brain regions with group ALFF differences showed significant correlations with the performance of cognitive function measured with MMSE, and with the emotion state measured with GD scale. Our results suggest that the ALFF measurement of intrinsic or spontaneous brain activity could be useful to characterize the early physiological changes of the EMCI stage of AD.

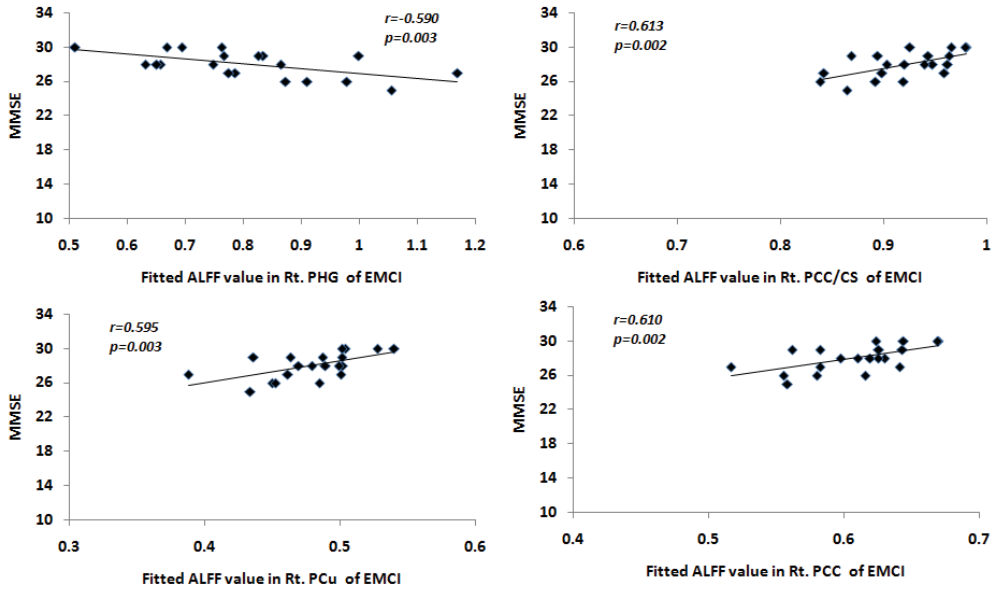

Fig. (7). MMSE showed significantly positive correlation with ALFF in three clusters located at right PCC/CS, PCu and PCC, while negative correlation with ALFF in a cluster of right PHG, for EMCI patients.

Decreased ALFF in EMCI, LMCI and AD

We found that EMCI, LMCI and AD patients all showed decreased ALFF in PCC extending into CS, and PCu extending into paracentral lobule (PCL), which were key DMN regions [28, 29]. DMN activity impairments were considered to be highly related to AD and MCI [18, 30]. Specifically, PCC always showed the most significant group differences between MCI/AD patients and controls, with a general pattern of AD < MCI < healthy elderly [14]. In the current study, the identified DMN regions showed a tendency of AD<LMCI<EMCI<NC, and right PCC was the maximum location with group difference using ANOCVA. It was also found that ALFF values in right PCC and PCu were significantly positively correlated with cognitive impairment as measured by MMSE for EMCI, LMCI and AD patients, but not for NC (Fig. **5-7**). These results further demonstrated the DMN abnormalities in AD and MCI [15-18, 31-35], and suggested that PCC ALFF activity might be a sensitive marker for early diagnosis of AD. Moreover, these findings might imply that the early diagnosis of AD could be advanced to an earlier stage of EMCI based on PCC activity.

We also found ALFF in thalamus was significantly reduced in three groups of patients with a linear pattern of AD<LMCI<EMCI<NC. This is consistent with the previous findings of altered thalamus functional connectivity [36, 37] in MCI and AD. Therefore, congruent with previous reports, it was postulated that the impaired thalamus may be related to cognitive dysfunction of patients, as ALFF in this regions is positively correlated with MMSE for LMCI. An alternative explanation was that the impairment of thalamus activity might be related to depression in patients, as all three groups of patients had significant depression symptoms (Table **1**), and ALFF in right thalamus was negatively correlated with GD scale both for EMCI and LMCI. We argued that the two explanations were not competitive, but might co-exist, because the thalamus complex is a critical component of the frontal cortical-basal ganglia-thalamic circuits that mediate motivation and emotional drive, planning and cognition for the development and expression of goal-directed behaviors [38].

LG was found to show decreased ALFF in patients with a general pattern of AD<LMCI<EMCI<NC. This is consistent with some previous findings in MCI and AD. For example, Using graph analysis, Yao *et al.* [39] found that, compared with NC, the nodal centrality of MCI and AD significantly decreased in the left LG and other regions, and compared with MCI, the nodal centrality in AD showed significant decreases in the right LG. Additionally, the present study found a significantly positive correlation between ALFF in right LG and MMSE for LMCI, and similar to EMCI and AD, although not significant. These results drive us to conclude that LG might be an important region reflects the cognitive impairment of EMCI, LMCI and AD.

Increased PHG ALFF in EMCI, LMCI and AD

We observed increased ALFF in right PHG for the three groups of patients with a linear tendency of AD>LMCI> EMCI>NC. This is congruent with previous reports that showed increased activation in PHG during episodic memory encoding [40] and a significant increase in the interregional correlations in PHG in MCI and AD, as compared with NC [39]. This phenomena may represent a compensatory process (i.e., increased neuronal recruitment) in the setting of early pathology. This explanation is reinforced by our observation that more severe cognitive deficits (measured by MMSE) are associated with higher ALFF values in PHG for EMCI. Would it be possible that increased ALFF in PHG will be more prominent in early MCI as a compensation mechanism? A long-term follow-up fMRI study of EMCI patients with a larger population is still required in the future.

Physiological Implications of ALFF Alterations in EMCI, LMCI and AD

ALFF is a data-derived measure, and its physiological significance is still unclear [10-11]. Recently, Li *et al.* [41] examined the cerebral blood flow (CBF) correlations of ALFF, and found that ALFF is highly and reliably correlated with CBF in most of brain cortex. These findings demonstrated that ALFF are coupled with regional CBF and are therefore linked to regional spontaneous brain activity. In terms of the apparent link between ALFF and CBF, this study is directly comparable with a previous arterial spin labeling (ASL) study. Using ASL, Wang *et al.* [42] also found a a gradually decreased CBF in controls, EMCI, LMCI, and AD in a predetermined set of regions, which is highly overlapped with the identified regions in this study. These findings suggested that the alterations in EMCI, LMCI and AD measured by using ALFF may reflect the CBF changes in these patients.

Limitations

There are still technical and biological limitations in the current study. First, the head motion of the participants may affect our results. However, the mean translation and roll rotation among the six translations and rotations parameters in x, y, or z directions show no significant differences among EMCI, LMCI, AD and NC ($p>0.1$). We also analyzed the data by taking the head-motion parameters as covariates, and found that the results remained nearly unchanged. It implies that our results were not significantly influenced by the head motion. Second, although the fMRI time series is band-pass filtered to reduce the effects of very low frequency and high frequency physiological noise including respiratory and aliased cardiac signals, it should be noted that the cardiac signals (about 1.3 Hz) cannot be removed completely with the longer TR (e.g., 2 s) acquisition according to the Nyquist-Shannon sampling theorem.

CONCLUSIONS

In this study, we provided evidence that EMCI, LMCI and AD patients had abnormal LFO amplitude in many brain regions, including PCC, PCu, thalamus, LG and PHG. These results extended our knowledge well beyond the previous MCI/AD-related findings, and suggested that ALFF measure is a useful bio-marker to detect the earlier AD changes in the EMCI stage. Thus, this study offers insights into understanding the disease progression of the brain's intrinsic activities from healthy elderly to those with EMCI, LMCI and AD.

CONFLICT OF INTEREST

The authors confirm that this article content has no conflicts of interest.

ACKNOWLEDGEMENTS

This work was supported by the Natural Science Foundation of China (Grant Nos. 61105118, 61373101), Beijing Nova Program (Z12111000250000, Z131107000413120), Open Research Fund of the State Key Laboratory of Cognitive Neuroscience and Learning (No. CNLZD1302), Open Research Fund of Zhejiang Key Laboratory for Research in Assessment of Cognitive Impairments. The funders had no role in study design, data collection and analysis, decision to publish, or preparation of the manuscript.

DISCLOSURE

Data used in the preparation of this article were obtained from the Alzheimer's Disease Neuroimaging Initiative (ADNI) database (www.loni.ucla.edu\ADNI). As such, the investigators within the ADNI contributed to the design and implementation of ADNI and/or provided data but did not participate in analysis or writing of this report. Complete listing of ADNI investigators is available at http://www.loni.ucla.edu/ADNI/Collaboration/ADNI_Authorship_ list.pdf

SUPPLEMENTARY MATERIALS

Supplementary material is available on the publisher's web site along with the published article.

REFERENCES

[1] Brookmeyer R, Johnson E, Ziegler-Graham K, Arrighi HM. Forecasting the global burden of Alzheimer's disease. Alzheimers Dement 3: 186-191 (2007).

[2] Leifer BP. Early diagnosis of Alzheimer's disease: clinical and economic benefits. J Am Geriatr Soc 51: S281-288 (2003).

[3] Petersen RC, Doody R, Kurz A, Mohs RC, Morris JC, Rabins PV, *et al.* Current concepts in mild cognitive impairment. Arch Neurol 58: 1985-1992 (2001).

[4] Aisen PS, Petersen RC, Donohue MC, Gamst A, Raman R, Thomas RG, *et al.* Clinical core of the Alzheimer's Disease Neuroimaging Initiative: progress and plans. Alzheimers Dement 6: 239-246 (2010).

[5] Weiner MW, Aisen PS, Jack CR Jr, Jagust WJ, Trojanowski JQ, Shaw L, *et al.* The Alzheimer's disease neuroimaging initiative: progress report and future plans. Alzheimers Dement 6: 202-211 (2010).

[6] Ewers M, Sperling RA, Klunk WE, Weiner MW, Hampel H. Neuroimaging markers for the prediction and early diagnosis of Alzheimer's disease dementia. Trends Neurosci 34: 430-442 (2011).

[7] Chhatwal JP, Sperling RA. Functional MRI of mnemonic networks across the spectrum of normal aging, mild cognitive impairment, and Alzheimer's disease. J Alzheimers Dis 3: S155-167 (2012).

[8] Vemuri P, Jones DT, Jack CR. Resting state functional MRI in Alzheimer's Disease. Alzheimer's Res Ther 4: 2-10 (2011).

[9] Fleisher AS, Sherzai A, Taylor C, Langbaum JB, Chen K, Buxton RB. Resting-state BOLD networks versus task-associated functional MRI for distinguishing Alzheimer's disease risk groups. Neuroimage 47(4): 1678-1690 (2009).

[10] Zang YF, He Y, Zhu CZ, Cao QJ, Sui MQ, Liang M, *et al.* Altered baseline brain activity in children with ADHD revealed by resting-state functional MRI. Brain Dev 29: 83-91 (2007).

[11] Zuo XN, Di Martino A, Kelly C, Shehzad ZE, Gee DG, Klein DF, *et al.* The oscillating brain: complex and reliable. Neuroimage 49: 1432-1445 (2010).

[12] Han Y, Wang JH, Zhao ZL, Min BQ, Lu J, Li KC, *et al.* Frequency-dependent changes in the amplitude of low-frequency fluctuations in amnestic mild cognitive impairment: A resting-state fMRI study. NeuroImage 55: 287-295 (2011).

[13] Xi Q, Zhao XH, Wang PJ, Guo QH, Yan CG, He Y. Functional MRI study of mild Alzheimer's disease using amplitude of low frequency fluctuation analysis. Chin Med J 125: 858-862 (2012).

[14] Wang ZQ, Yan CG, Zhao C, Qi ZG, Zhou WD, Lu J, *et al.* Spatial patterns of intrinsic brain activity in mild cognitive impairment and Alzheimer's disease: A resting-state functional MRI study. Human Brain Mapping 32: 1720-1740 (2011).

[15] Sorg C, Riedl V, Muhlau M, Calhoun VD, Eichele T, Läer L, *et al.* Selective changes of resting-state networks in individuals at risk for Alzheimer's disease. Proc Natl Acad Sci USA 104: 18760-18765 (2007).

[16] Bai F, Zhang Z, Yu H, Shi Y, Yuan Y, Zhu W, *et al.* Default-mode network activity distinguishes amnestic type mild cognitive impairment from healthy aging: a combined structural and resting-state functional MRI study. Neurosci Letters 438: 111-115 (2008).

[17] Bai F, Watson DR, Yu H, Shi Y, Yuan Y, Zhang Z. Abnormal resting-state functional connectivity of posterior cingulate cortex in amnestic type mild cognitive impairment. Brain Res 1302: 167-174 (2009).

[18] Greicius MD, Srivastava G, Reiss AL, Menon V. Default-mode network activity distinguishes Alzheimer's disease from healthy aging: evidence from functional MRI. Proc Natl Acad Sci USA 101: 4637-4642 (2004).

[19] He Y, Wang L, Zang Y, Tian L, Zhang X, Li K, *et al.* Regional coherence changes in the early stages of Alzheimer's disease: a combined structural and resting-state functional MRI study. Neuroimage 35: 488-500 (2007).

[20] Zhang HY, Wang SJ, Xing J, Liu B, Ma ZL, Yang M, *et al.* Detection of PCC functional connectivity characteristics in resting-state fMRI in mild Alzheimer's disease. Behav Brain Res 197: 103-108 (2009).

[21] Yan CG, Zang YF. DPARSF: A MATLAB toolbox for "Pipeline" data analysis of resting-state fMRI. Front Syst Neurosci 4: 13 (2010).

[22] Ashburner J, Friston KJ. Unified segmentation. NeuroImage 26: 839-851 (2005).

[23] Grecius M, Krasnow B, Reiss A, Menon V. Functional connectivity in the resting brain: a network analysis of the default mode hypothesis. Proc Natl Acad Sci USA 100: 253-258 (2003).

[24] Song XW, Dong ZY, Long XY, Li SF, Zuo XN, Zhu CZ, *et al.* REST: a toolkit for resting-state functional magnetic resonance imaging data processing. PLoS One 6: e25031 (2011).

[25] Hoptman MJ, Zuo XN, Butler PD, Javitt DC, D'Angelo D, Mauro CJ, *et al.* Amplitude of low-frequency oscillations in schizophrenia: a resting state fMRI study. Schizophr Res 117: 13-20 (2010).

[26] Bokde AL, Pietrini P, Ibanez V, Furey ML, Alexander GE, Graff-Radford NR, *et al.* The effect of brain atrophy on cerebral hypometabolism in the visual variant of Alzheimer disease. Arch Neurol 58: 480-486 (2001).

[27] Collignon A, Maes F, Delaere D, Vandermeulen D, Suetens P, Marchal G. Automated multi-modality image registration based on information theory. In (Eds: Bizais Y, Barillot C, Di Paola R) Information Processing in Medical Imaging. Dordrecht (The Netherlands): Kluwer Academic Publishers pp. 263-274 (1995).

[28] Raichle ME, MacLeod AM, Snyder AZ, Powers WJ, Gusnard DA, Shulman GL. A default mode of brain function. Proc Natl Acad Sci USA 98: 676-682 (2001).

[29] Mason MF, Norton MI, Van Horn JD, Wegner DM, Grafton ST, Macrae CN. Wandering minds: the default network and stimulus-independent thought. Science 315: 393-395 (2007).

[30] Broyd SJ, Demanuele C, Debener S, Helps SK, James CJ, Sonuga-Barke EJ. Default-mode brain dysfunction in mental disorders: A systematic review. Neurosci Biobehav Rev 33(3): 279-296 (2009).

[31] Bai F, Watson DR, Shi Y, Wang Y, Yue C, Teng YH, *et al.* Specifically progressive deficits of brain functional marker in amnestic type mild cognitive impairment. PLoS One 6: e24271 (2011).

[32] Qi Z, Wu X, Wang Z, Zhang N, Dong H, Yao L, *et al.* Impairment and compensation coexist in amnestic MCI default mode network. Neuroimage 50(1): 48-55 (2010).

[33] Liang P, Wang Z, Yang Y, Jia X, Li K. Functional disconnection and compensation in mild cognitive impairment: Evidence from DLPFC connectivity using resting-state fMRI. PLoS ONE 6: e22153 (2011).

[34] Liang P, Wang Z, Yang Y, Li K. Three subsystems of the inferior parietal cortex are differently affected in mild cognitive impairment. J Alzheimer's Disease 30(3): 475-487 (2012).

[35] Liang P, Li Z, Deshpande G, Wang Z, Hu X, Li KC. Altered causal connectivity of resting state brain networks in amnesic MCI. PLoS ONE 9(3): e88476 (2014).

[36] Wang Z, Jia X, Liang P, Qi Z, Yang Y, Zhou W, *et al.* Changes in thalamus connectivity in mild cognitive impairment: evidence from resting state fMRI. Eur J Radiol 81: 277-285 (2012).

[37] Zhou B, Liu Y, Zhang Z, An N, Yao H, Wang P, *et al.* Impaired functional connectivity of the thalamus in alzheimer' s disease and mild cognitive impairment: a resting-state fMRI study. Curr Alzheimer Res 10: 754-766 (2013).

[38] Haber SN, Calzavara R. The cortico-basal ganglia integrative network: the role of the thalamus. Brain Res Bull 78: 69-74 (2009).

[39] Yao Z, Zhang Y, Lin L, Zhou Y, Xu C, Jiang T*, et al.* Abnormal cortical networks in mild cognitive impairment and Alzheimer's disease. PLoS Comput Biol 6: e1001006 (2010).

[40] Dickerson BC, Salat DH, Bates JF, Atiya M, Killiany RJ, Greve DN, *et al.* Medial temporal lobe function and structure in mild cognitive impairment. Ann Neurol 56: 27-35 (2004).

[41] Li Z, Zhu Y, Childress AR, Detre JA, Wang Z. Relations between BOLD fMRI-derived resting brain activity and cerebral blood flow. PLoS ONE 7: e44556 (2012).

[42] Wang Z, Das SR, Xie SX, Arnold SE, Detre JA, Wolk DA, *et al.* Arterial spin labeled MRI in prodromal Alzheimer's disease: A multi-site study. Neuroimage Clin 2: 630-636 (2013).

Received: October 07, 2013 **Revised: February 17, 2014** **Accepted: March 17, 2014**